# Independent Component Analysis for Clutter Reduction in Ground Penetrating Radar Data

Brian Karlsen[a], Helge B.D. Sørensen[a], Jan Larsen[b] and Kaj B. Jakobsen[a]

[a]Ørsted•DTU, Technical University of Denmark
Ørsteds Plads, Building 348, DK-2800 Kongens Lyngby, Denmark

[b]Informatics and Mathematical Modelling, Technical University of Denmark
Richard Petersens Plads, Building 321, DK-2800 Kongens Lyngby, Denmark.

## ABSTRACT

Statistical signal processing approaches based on Independent Component Analysis (ICA) algorithms for clutter reduction in Stepped-Frequency Ground Penetrating Radar (SF-GPR) data are presented. The purpose of the clutter reduction is indirectly to decompose the GPR data into clutter reduced GPR data and clutter. The experiments indicate that ICA algorithms can decompose GPR data into suitable subspace components, which makes it possible to select a subset of components containing primarily target information (like anti-personal landmines) and others which contain mainly clutter information. The paper compares spatial and temporal ICA approaches on field-test data from shallow buried iron and plastic anti-personal landmine dummies. The data are acquired using a monostatic bow-tie antenna operating in the frequency range from 500 MHz to 2.5 GHz.

**Keywords:** Anti-personal landmine detection, ground penetrating radar, independent component analysis, statistical signal processing, clutter reduction.

## 1. INTRODUCTION

The Ground Penetrating Radar (GPR) is widely used in the application of detection of landmines. The advantage of using a GPR is given by the fact that a GPR is able to detect buried objects in the received electromagnetic fields scattered from the ground. This property makes the GPR able to detect landmines, and in particular anti-personal landmines of plastic with a low content of metal[1,2]. Mostly, those kinds of landmines are buried close to the surface of the ground, where the detection of objects is very weak due to the strong clutter scattering from the ground surface. Clutter hampers the detection of the landmines and therefore gives a significant problem for automatic landmine detection systems. In general, the clutter that effects a GPR can be defined as those signals that are unrelated to the target scattering characteristics but occupy the same frequency band as the targets. Clutter can be caused by multiple reflections, e.g., in the antenna, between the antenna and the ground surface, and the non-mine targets buried in the ground. However, on the detection of shallow buried landmines the ground surface clutter is the strongest and most significant clutter. To increase the detection of shallow buried objects it is therefore necessary to deploy proper ground surface clutter reduction methods on the GPR signals to enhance the detection of shallow buried landmines.

The literature suggests a number of clutter reduction methods, such as likelihood ratio testing[3], parametric system identification[4–7], wavelet packet decomposition[8,9], subspace techniques[10–14], and simple mean subtraction[1]. However, many of these fail to detect shallow buried landmines, mostly because of the statistical nature of the clutter, e.g., the ground surface is not perfectly flat or even relative smooth. Another problem is that many of the methods use reference signal estimates of the signature of a landmine. These reference signals are used to remove signal that are unrelated to the reference. However, a target signal which has little correlation with the reference signals may not be detected, hence, be classified as clutter.

Further author information on: *BK*: brk@oersted.dtu.dk, www.oersted.dtu.dk; *HBDS*: hbs@oersted.dtu.dk, www.oersted.dtu.dk; *JL*: jl@imm.dtu.dk, www.imm.dtu.dk/~jl; *KBJ*: kbj@oersted.dtu.dk, www.oersted.dtu.dk

To reduce the clutter we have suggested another promising approach[11,12] based on decomposition of the GPR signals into clutter and landmine signals using Principal Component Analysis (PCA) and Independent Component Analysis (ICA). In this work we focus on reducing the ground surface clutter using statistical unsupervised learning methods based on spatial and temporal ICA. The basic idea using ICA is to decompose the received GPR signals into subspaces of clutter signals and landmine signals, respectively. Previous work[12] addressed the use of temporal ICA only.

In this paper we extent the work by considering spatial ICA and more elaborate experimental studies. Section 2 presents the spatial and temporal ICA based clutter reduction methods and section 3 describes for selecting of relevant ICA components. Finally, section 4 provides a comparative study of the presented methods, which are tested on GPR-data collected at an indoor GPR measurement facility at the Technical University of Denmark.

## 2. CLUTTER REDUCTION USING INDEPENDENT COMPONENT ANALYSIS

To reduce the clutter in the GPR data we focus on unsupervised statistical methods based on spatial and temporal Independent Component Analysis (s-ICA and t-ICA). The s-ICA and t-ICA method are two complementary ways to subspace decompose a multi-channel signal into a set of weighting vectors (eigenimages) and a associated set of time signals using ICA[15–17]. The s-ICA and t-ICA method are inspired by a recently suggested clutter reduction method based on Principal Component Analysis (PCA[11,12]). The s-ICA and t-ICA method for clutter reduction resembles that of the PCA method. The major difference is that the subspace formed by ICA is not orthogonal as in PCA. Moreover, the independent components (IC's), which are the counterparts of the Principal Components (PC's), are statistically independent. We thus expect the IC's to have a more distinct time and spatial localization. From recently presented work[12], t-ICA clearly shows a more distinct time localization than PCA. Briefly, the s-ICA and t-ICA basically decomposes GPR signals into a set of eigenimages and associated time signals. The s-ICA finds independent eigenimages and a associated set of time signals, whereas the t-ICA finds independent time signals and a associated set of eigenimages. From the s-ICA and t-ICA, clutter reduction is then obtained by selecting components, which contain landmine-like signatures only.

To employ the ICA subspace decomposition methods on the GPR data, a signal space must be defined. The space observed is spanned by the multi-channel GPR time-domain signals as expressed by the signal matrix $\boldsymbol{X} \in \mathbb{R}^{P \times N}$ expressed by

$$\boldsymbol{X} = \{X_{p,n}\} = \{x_p(n)\} = \{x_{i,j}(n)\} = [\boldsymbol{x}(1), \boldsymbol{x}(2), \cdots, \boldsymbol{x}(N)], \tag{1}$$

where $P$ is the number of time-domain signals, which are received by scanning the GPR above the ground surface in the $x$- and $y$-direction, $N$ is the number of samples in each of the received time-domain signals, and $x_{i,j}(n)$ is the time-domain signal received at the antenna located at position $\big(x,y\big) = \big(x = (i-1)\triangle x, y = (j-1)\triangle y\big)$, where $i = 1, 2, \cdots, I$, and $j = 1, 2, \cdots, J$. $\triangle x$ and $\triangle y$ are the antenna location step size in the $x$- and $y$-direction, respectively, and $p = i + (j-1)I$. $I$ and $J$ is the number of antenna locations in the $x$- and $y$-direction, respectively. In general we expect that the mean value of $\boldsymbol{X}$ is equal zero, $E\{\boldsymbol{X}\} = 0$. Hence, we may redefine $x_p(n)$ to $x_p(n) = \bar{x}_{i,j}(n)$, where

$$x_p(n) = \bar{x}_{i,j}(n) = x_{i,j}(n) - \frac{1}{IJ}\sum_{i=1}^{I}\sum_{j=1}^{J} x_{i,j}(n), \quad p = i + (j-1)I, \quad i \in [1;I], \quad j \in [1;J], \quad p \in [i;JI] \tag{2}$$

That is, in the signal matrix $\boldsymbol{X}$, i.e., $x_p(n)$, $n = 1, 2, \cdots, N$, is the $p$'th received time-domain signal, or in practice, the $p$'th received time-domain signal subtracted by the mean value of the ensemble of received time-domain signals. Equation 2 is also known as the mean-subtraction clutter reduction method[1].

***PCA***. In order to compare and in order to provide at reduced rank data set[19,20] as input to the s-ICA and t-ICA, we first employ the PCA on the data set. PCA was executed using singular value decomposition (SVD),

$$\boldsymbol{X} = \boldsymbol{U}\boldsymbol{D}\boldsymbol{V}^{\top} = \sum_{i=1}^{N} \boldsymbol{u}_i D_{i,i} \boldsymbol{v}_i^{\top} \quad , \quad X_{p,n} = \sum_{i=1}^{N} U_{p,i} D_{i,i} V_{n,i} \tag{3}$$

where the $P \times N$ matrix $\boldsymbol{U} = \{U_{p,i}\} = [\boldsymbol{u}_1, \boldsymbol{u}_2, \cdots, \boldsymbol{u}_N]$ and the $N \times N$ matrix $\boldsymbol{V} = \{V_{n,i}\} = [\boldsymbol{v}_1, \boldsymbol{v}_2, \cdots, \boldsymbol{v}_N]$ represent orthonormal basis vectors, i.e., eigenvectors of the symmetric matrices $\boldsymbol{X}\boldsymbol{X}^{\mathrm{T}}$ and $\boldsymbol{X}^{\mathrm{T}}\boldsymbol{X}$, respectively. $\boldsymbol{D} = D_{i,i}$ is an $N \times N$ diagonal matrix of singular values ranked in decreasing order, as shown by $D_{i-1,i-1} \geq D_{i,i}, \forall i \in [2; N]$. The SVD identifies a set of uncorrelated time signals, the principal components (PC's): $\boldsymbol{y}_i = D_{i,i}\boldsymbol{v}_i$, enumerated by the component index $i = 1, 2, \ldots, N$ and $\boldsymbol{y}_i = [y_i(1), \cdots, y_i(N)]^\top$. That is, from the PCA we can write the observed signal matrix as a weighted sum of fixed eigenvectors (eigenimages), $\boldsymbol{u}_i$, that often lend themselves into direct interpretation. The PC's and the eigenimages are used as inputs to the t-ICA and s-ICA, respectively. The dimension of the PCA data set will be $d \leq N$. That is, we model $\boldsymbol{X}$ only from non-zero eigenvalues[20].

***Temporal ICA***. t-ICA embodies the assumption that each PC, $\boldsymbol{y}_i$, is a linear combination of $M$ temporal independent time signals, the IC's. The t-ICA is processed in two steps. First, $\boldsymbol{X}$ is projected to a subspace spanned by $M$, $M \leq d$, selected PC's., e.g., the first $M$ PC's. That is, $\boldsymbol{Y} = \widetilde{\boldsymbol{U}}^\top \boldsymbol{X}$, where $\widetilde{\boldsymbol{U}} = [\boldsymbol{u}_1, \boldsymbol{u}_2, \cdots, \boldsymbol{u}_M]$ and $\boldsymbol{Y}$ is an $M \times N$ matrix, $\boldsymbol{Y} = [\boldsymbol{y}_1, \boldsymbol{y}_2, \cdots, \boldsymbol{y}_m]^\top$. Hence, the t-ICA problem is defined as

$$\boldsymbol{Y} = \boldsymbol{A}_t \boldsymbol{S}_t, \tag{4}$$

where $\boldsymbol{A}_t$ is the $M \times M$ matrix of mixing coefficients and $\boldsymbol{S}_t$ is the $M \times N$ matrix of independent time signals, (IC's). Secondly, the mixing matrix, $\boldsymbol{A}_t$, and the matrix of independent time series, $\boldsymbol{S}_t$, are estimated[16,17]. The original signal matrix is reconstructed as $\widehat{\boldsymbol{X}} = \boldsymbol{W}_t \boldsymbol{S}_t = \sum_{i=1}^{M} \boldsymbol{w}_{t_i} \boldsymbol{s}_{t_i}$, where $\boldsymbol{W}_t = \widetilde{\boldsymbol{U}}\boldsymbol{A}_t$ is the matrix of eigenimages. $\boldsymbol{s}_{t_i} = [s_{t_i}(1), \cdots, s_{t_i}(N)]$ and $\boldsymbol{w}_{t_i} = [w_{t_i}(1), \cdots, w_{t_i}(P)]^\top$ is the $i$'th independent time signal and associated eigenimage, respectively. From the t-ICA clutter reduction can then be obtained by selecting components which mainly contain landmine-like signatures and then reconstruct the signal matrix, $\widehat{\boldsymbol{X}}$. A more detailed description of this procedure is given in Section 3.

***Spatial ICA***. s-ICA embodies the assumption that each eigenimage, $\boldsymbol{u}_i$, is composed of a linear combination of $M$ spatially IC eigenimages. The s-ICA is done in two steps. First is $\boldsymbol{X}$ projected to a subspace spanned by $M$ selected PC's., e.g., the first $M$ PC's, i.e., similar to the t-ICA, where we get $\boldsymbol{Y}$ and have $\widetilde{\boldsymbol{U}}$. Then, the s-ICA problem is defined as

$$\widetilde{\boldsymbol{U}}^\top = \boldsymbol{A}_s \boldsymbol{S}_s, \tag{5}$$

where $\boldsymbol{A}_s$ is the $M \times M$ matrix of mixing coefficients and $\boldsymbol{S}_s$ is the $M \times P$ matrix of independent eigenimages, IC's. Secondly, the mixing matrix, $\boldsymbol{A}_s$, and the matrix of independent eigenimages, $\boldsymbol{S}_s$, are estimated[16,17] in a similar way as for the t-ICA. The original signal matrix is reconstructed as $\widehat{\boldsymbol{X}}^\top = \boldsymbol{W}_s \boldsymbol{S}_s = \sum_{i=1}^{M} \boldsymbol{w}_{s_i} \boldsymbol{s}_{s_i}$, where $\boldsymbol{W}_s = \boldsymbol{Y}\boldsymbol{A}_s$ is the matrix of time signals. $\boldsymbol{s}_{s_i} = [s_{s_i}(1), \cdots, s_{s_i}(P)]$ and $\boldsymbol{w}_{s_i} = [w_{s_i}(1), \cdots, w_{s_i}(N)]^\top$ is the $i$'th independent eigenimage and associated time signal, respectively. s-ICA clutter reduction resembles that of the t-ICA clutter reduction (refer to Section 3).

But how do we get $\boldsymbol{A}_s$, $\boldsymbol{A}_t$, $\boldsymbol{S}_s$ and $\boldsymbol{S}_t$? The literature provides a number of algorithms for estimating the $\boldsymbol{A}$ mixing matrix and the $\boldsymbol{S}$ source matrix*. Basically they can be divided into two families in which the first deploy higher (or lower) order moments of non-Gaussian sources, whereas the other family uses the time correlation of the source signals. In the present case we expect that the sources are both non-Gaussian and colored. We deploy a member from the first family: the widely used Bell-Sejnowski[16] algorithm using natural gradient learning.

## 3. SELECTION OF COMPONENTS AND RECONSTRUCTION

The clutter reduction is obtained by selecting components that have landmine-like signatures only. The features we can base our selection on are temporal features and spatial features. We suggest three selection methods, which are based on temporal features, spatial features, and combined temporal and spatial features.

***Temporal Features***: selecting components only using information from $\boldsymbol{W}_s$ and $\boldsymbol{S}_t$. Consider the projection onto the subspace spanned by $K$ selected time signals which mainly contain information about the

*For a resent review the reader is referred to[21].

landmine object, i.e., $\boldsymbol{W}_t = \boldsymbol{X}\widetilde{\boldsymbol{S}}_t^{\top}$, $\widetilde{\boldsymbol{S}}_t = [\boldsymbol{s}_{t_{i_1}}, \boldsymbol{s}_{t_{i_2}}, \cdots, \boldsymbol{s}_{t_{i_K}}]^{\top}$ for the t-ICA, and $\boldsymbol{S}_s = \widetilde{\boldsymbol{W}}_s^{\top}\boldsymbol{X}^{\top}$, $\widetilde{\boldsymbol{W}}_s = [\boldsymbol{w}_{s_{i_1}}, \boldsymbol{w}_{s_{i_2}}, \cdots, \boldsymbol{w}_{s_{i_K}}]$ for the s-ICA. The selection of the components can be done by inspecting the time signals only. If we know were the ground surface is located in time, we then remove those time signal components that peaks before and at the ground surface. The clutter is subsequently reduced by reconstructing $\boldsymbol{X}$ from the subspace as given by

$$\widehat{\boldsymbol{X}} = \boldsymbol{W}_t\widetilde{\boldsymbol{S}}_t \quad , \quad \widehat{\boldsymbol{X}}^{\top} = \widetilde{\boldsymbol{W}}_s\boldsymbol{S}_s \tag{6}$$

for t-ICA and s-ICA, respectively.

***Spatial Features***. Selecting components only using information from $\boldsymbol{W}_t$ and $\boldsymbol{S}_s$. Consider the projection onto the subspace spanned by $K$ selected eigenimages which mainly contain information about the landmine object, i.e., $\boldsymbol{S}_t = \widetilde{\boldsymbol{W}}_t^{\top}\boldsymbol{X}$, $\widetilde{\boldsymbol{W}}_t = [\boldsymbol{w}_{t_{i_1}}, \boldsymbol{w}_{t_{i_2}}, \cdots, \boldsymbol{w}_{t_{i_K}}]$ for the t-ICA, and $\boldsymbol{W}_s = \boldsymbol{X}^{\top}\widetilde{\boldsymbol{S}}_s^{\top}$, $\widetilde{\boldsymbol{S}}_s = [\boldsymbol{s}_{s_{i_1}}, \boldsymbol{s}_{s_{i_2}}, \cdots, \boldsymbol{s}_{s_{i_K}}]^{\top}$ for the s-ICA. The selection of the components can be done by inspecting the eigenimages only. We then remove those components that show no spatial landmine-like signatures. The clutter is subsequently reduced by reconstructing $\boldsymbol{X}$ from the subspace as given by

$$\widehat{\boldsymbol{X}} = \widetilde{\boldsymbol{W}}_t\boldsymbol{S}_t \quad , \quad \widehat{\boldsymbol{X}}^{\top} = \boldsymbol{W}_s\widetilde{\boldsymbol{S}}_s \tag{7}$$

for t-ICA and s-ICA, respectively.

***Spatial Temporal Features***. Selecting components only using information from $\boldsymbol{W}_s$ and $\boldsymbol{S}_t$, $\boldsymbol{W}_t$, and $\boldsymbol{S}_s$. That is, selection of components that shows both temporal and spatial landmine-like signatures. Consider a subspace spanned by $K$ components as in the spatial and the temporal feature selection methods. Then we select components that show landmine-like signatures in both eigenimages and time signals. The clutter is subsequently reduced by reconstructing $\boldsymbol{X}$ from the subspace as expressed by equation 6 and 7.

The overall objective of the ICA methods is automatic detection of the landmines by automatic selection of the components based on $\boldsymbol{W_s}$, $\boldsymbol{S_s}$, $\boldsymbol{W_t}$, and $\boldsymbol{S_t}$. However, this work is done on a very small data set. Therefore, the selection of the components is done by visual inspection of eigenimages and time signals.

## 4. CASE STUDY: M56 IRON AND PLASTIC LANDMINE DUMMIES

The comparative study of the t-ICA and s-ICA methods for clutter reduction in GPR data was performed on field-test Stepped-Frequency GPR data. The field-test data was collected using a monostatic bow-tie antenna operating in the frequency range from 500 MHz to 2.5 GHz. The data was acquired using a HP8753A network analyzer. The bandwidth of the antenna determines the resolution, which is approximately 7.5 cm in free-space. The frequency-domain data was Fourier transformed to the time-domain using a sampling frequency of 10.24 GHz, which corresponds to a free-space sampling of 2.9 cm in the depth direction, which is below the resolution set by the antenna bandwidth. In a measurement area of 126 cm $\times$ 90 cm M56 landmine dummies of iron and plastic (filled with bees wax) were buried in the center of the field in relative wet soil 5 cm below the surface. The dimension of the landmine dummies are: diameter 5.4 cm, and height 4 cm. The measurement area was scanned so every antenna positions were located ($\triangle x = 1$ cm) $\times$ ($\triangle y = 1$ cm) from each other.

In Figure 1 and Figure 2 are the PCA results shown. The Figures show the first $M = 21$ eigenimages, $\boldsymbol{u}_i$, $i = 1, 2, \ldots, M$, and associated PC's, $\boldsymbol{y}_i$, $i = 1, 2, \ldots, M$, for the iron dummy and the plastic dummy, respectively. In total we got $d = 24$ and $d = 23$ eigenimages and associated PC's for the iron dummy and for the plastic dummy, respectively. However, the last eigenimages and PC's shows only noise-like textures, as also are shown from the first 21 eigenimages and PC's due to the fact that the later eigenimages and PC's shows noise-like texture only. All the components are sorted after variance. That is, the first component contributes most to $\boldsymbol{X}$, where as the last component has the lowest contribution to $\boldsymbol{X}$. The variance is given by $D_{i,i}$ for the $i$'th component. For the signal matrix, $\boldsymbol{X}$, we have $P = 127 \times 91 = 11557$ antenna positions. That is, $P$ received time-domain signals at $P$ locations. The number of samples, $\boldsymbol{N}$, was 62. The eigenimages and PC's are used as inputs to the s-ICA and t-ICA methods.

The PCA end up with a data set of dimension $d = 24$ and $d = 23$ for the iron and plastic dummy, respectively. The higher the dimension, $d$, is, a higher number of components to select exist. Further, the time-domain signals

from one landmine may be spread out in more than one component. This makes the selection of components rather complex. The solution to this is to *compress* the information into fewer components. That is, having a subspace decomposition method that is able to lower the dimension of the data set without loosing information, e.g., a subspace decomposition method that seeks the most optimal dimension. However, the Bell–Sejnowski ICA (BS-ICA) is not able to reduce the dimension of the data set in that way. Therefore, one way to reduce the number of dimensions is to reduce the number of inputs, with the cost of information. In order to see how the ICA performs on smaller subspaces, e.g., is it possible to *compress* the landmine-like signatures into fewer components, the t-ICA and s-ICA were tested on subspaces using the first $M = 15$, $M = 10$, and $M = 5$ eigenimages, $\boldsymbol{u}_i$, and associated PC's, $\boldsymbol{y}_i$. These eigenimages and PC's were selected due to the fact that later eigenimages and PC's than $M = 15$ shows only clutter-like signatures and that the contribution from those components in $\boldsymbol{X}$ is small (low variance).

In Figure 3 and Figure 4 are shown the first 12 components from the t-ICA and s-ICA using the first $M = 15$ PC's, $\widetilde{\boldsymbol{Y}} = [\boldsymbol{y}_1, \boldsymbol{y}_2, \cdots, \boldsymbol{y}_{15}]^\top$, as input to the t-ICA and first $M = 15$ eigenimages, $\widetilde{\boldsymbol{U}} = [\boldsymbol{u}_1, \boldsymbol{u}_2, \cdots, \boldsymbol{u}_{15}]$, as input to the s-ICA. In Figure 3 some of the eigenimages of the iron dummy experiments shows strong landmine-signatures, in particular eigenimage number 5 and 6 for the t-ICA and number 6 for the s-ICA. However, the signatures are more clearly pronounced for the s-ICA. Further, fewer eigenimages for the s-ICA shows landmine-like signatures. That is, the t-ICA spread the landmine information out in many components, whereas the s-ICA is able to compress the information in to few components. The time signals shows better localization for the t-ICA than for the s-ICA. That is, for the t-ICA the eigenimages can be associated with a particular depth. From the results it is shown that the t-ICA provides a better time separation, whereas the s-ICA provides at better spatial separation. For the M56 plastic dummy results, shown in Figure 4, similar results are obtained. However, the landmine-signature is less pronounced due to the low scatter from the landmine.

In Figure 5 to Figure 7 are the results of the clutter reduction shown. The images shows the total power of the first 30 samples of the received GPR time signal at each antenna location. That is, $\widehat{X}_{p_{pow}} = \sum_{n=l}^{L} \hat{x}_{p,n}^2$. The power is calculated using a rectangular window of size $L = 30$. By using the window size $L = 30$, we cover the area from the input of the antenna to approx. 20 cm under the ground surface. From the results in general it is clear that the selection method based on combined spatial and temporal features gives the best performance, particular when choosing $M = 15$ components. It is also shown that the t-ICA has a better performance than the s-ICA, when using only temporal features, and the s-ICA has better performance when using only spatial features. This is true for both the iron dummy and plastic dummy. However for the plastic dummy the best result is obtained when choosing a subspace of $M = 5$ components. Why the performance is poor at small subspaces may be found in the simple way we select the inputs to the s-ICA and t-ICA. From Figure 1 and Figure 2 it is clear that most of the landmine information is in component 5 to 12. By removing those components, which we do when we select the first $M = 5$ components, we will loose information. In Figure 6 and Figure 7 are mesh plots shown, they clearly shows that the clutter is reduced in the GPR data.

## 5. CONCLUSION

This paper provided a comparative study of spatial and temporal ICA for clutter reduction. The ICA methods were based on the Bell–Sejnowski ICA. From the results we have that the t-ICA provides more peaky time signals than the s-ICA, due to the fact that the t-ICA gives independent time signals. Hence, the t-ICA shows better performance in time localization. However, s-ICA shows more landmine-like eigenimages than the t-ICA, due to the fact that the eigenimages are independent in the s-ICA. Hence, s-ICA shows better performance in spatial localization. Three component selection methods were suggested and compared. They were base on temporal feature selection, spatial feature selection, and combined spatial and temporal feature selection. The combined showed best performance. That is, the best clutter reduction is obtain by selecting components were both eigenimages and associated time signals shows landmine-like signatures. Future studies will concentrate on ICA methods based on both spatial and temporal features and methods for automatic component selection.

## 6. ACKNOWLEDGEMENT

We thank Ole Nymann for enthusiastic and steady support of our work in humanitarian landmine detection. Furthermore, Peter Meincke is acknowledged for collaboration on field data acquisition.

## REFERENCES


1. D.J. Daniels: *Surface Penetrating Radar*, IEE, 1996.
2. H.B.D. Sørensen, K.B. Jakobsen and O. Nymann: "Identification of mine-shaped objects based on an efficient phase stepped-frequency radar approach" in *Proc. IEEE Image Processing* 1997, 3, 142 -145.
3. H. Brunzell: "Clutter Reduction and Object Detection in Surface Penetrating Radar," in *Proc. of IEE Radar'97*, issue 449, 1997, pp. 688–691.
4. J.W. Brooks, L. van Kempen & H. Sahli: "Primary Study in Adaptive Clutter Reduction and Buried Minelike Target Enhancement from GPR Data," in *Proc. of SPIE, AeroSense 2000: Detect. and Rem. Techn. for Mines and Minelike Targets V*, vol. 4038, 2000, pp. 1183–1192.
5. L. van Kempen, H. Sahli, E. Nyssen & J. Cornelis: "Signal Processing and Pattern Recognition Methods for Radar AP Mine Detection and Indentification," *Detect. of Aband. Land Mines*, no. 458, pp. 81–85, 1998.
6. A. van der Merwe & I.J. Gupta: "A Novel Signal Processing Technique for Clutter Reduction in GPR Measurements of Small, Shallow Land Mines," *IEEE Transactions on Geoscience and Remote Sensing* vol. 38, no. 6 , Nov. 2000, pp. 2627–2637.
7. J.L. Salvati, C.C. Chen & J.T. Johnson: "Theoretical Study of a Surface Clutter Reduction Algorithm," in *Proc. of 1998 IEEE International Geoscience and Remote Sensing*, vol. 3, 1998, pp. 1460–1462.
8. D. Carevic: "Clutter Reduction and Target Detection in Ground Penetrating Radar Data Using Wavelets," in *Proc. of SPIE Conf. on Detect. and Rem. Techn. for Mines and Minelike Targets IV*, vol. 3710, 1999, pp. 973–97.
9. H. Deng & H. Ling: "Clutter Reduction for Synthetic Aperture Radar Images Using Adaptive Wavelet Packet Transform," in *Proc. of IEEE Int. Ant. and Propaga. Soc. Symp.*, vol. 3, 1999, pp. 1780–1783.
10. A.H. Gynatilaka & B.A. Baertlein: "A subspace decomposition technique to improve GPR imaging of anti-personnel mines," in *Proc. of SPIE, AeroSense 2000: Detect. and Rem. Techn. for Mines and Minelike Targets V*, vol. 4038, 2000, pp. 1008–1018.
11. B. Karlsen, J. Larsen, K.B. Jakobsen, H.B.D. Sørensen & S. Abrahamson: "Antenna Characteristics and Air-Ground Interface Deembedding Methods for Stepped-Frequency Ground Penetrating Radar Measurements," in *Proc. of SPIE, AeroSense 2000: Detect. and Rem. Techn. for Mines and Minelike Targets V*, vol. 4038, 2000, pp. 1420–1430.
12. B. Karlsen, J. Larsen, H.B.D. Sørensen and K.B. Jakobsen: "Comparison of PCA and ICA based Clutter Reduction in GPR Systems for Anti-Personal Landmine Detection," in *Proc. of 11th IEEE Workshop on Statistical Signal Processing*, Singapore, Aug. 6–8, 2001, pp. 146–149.
13. A.K. Shaw & V. Bhatnagar: "Automatic Target Recognition Using Eigen-Templates," in *Proc. of SPIE Conference on Algorithms for Synthetic Aperture Radar Imagery V*, vol. 3370, 1998, pp. 448-459.
14. S.H. Yu & T.R. Witten: "Automatic Mine Detection based on Ground Penetratinig Radar," in *Proc. of SPIE Conference on Detect. and Rem. Techn. for Mines and Minelike Targets IV*, vol. 3710, 1999, pp. 961–972.
15. P. Comon: "Independent Component Analysis: A New Concept," *Sig. Proces.*, vol. 36, pp. 287–314, 1994.
16. A. Bell & T.J. Sejnowski: "An Information-Maximation Approach to Blind Separation and Blind Deconvelution," *Neural Computation*, vol. 7, pp. 1129–1159, 1995.
17. L. Molgedey & H. Schuster: "Separation of Independent Signals using Time-Delayed Correlations," *Physical Review Letters*, vol. 72, no. 23, pp. 3634–3637, 1994.
18. L.K. Hansen, J. Larsen & T. Kolenda: "On Independent Component Analysis for Multimedia Signals," in L. Guan, S.Y. Kung & J. Larsen (eds.) *Multimedia Image and Video Processing*, CRC Press, Ch. 7, pp. 175–199, 2000.
19. L.K. Hansen, J. Larsen & T. Kolenda: "Blind Detection of Independent Dynamic Components," in *Proc. IEEE ICASSP'2001*, Salt Lake City, SAM-P8.10, vol. 5, 2001.
20. B. Lautrup, L.K. Hansen, I. Law, N. Mørch, C. Svarer & S.C. Strother: "Massive weight sharing: A Cure for Extremely Ill-posed Problems," in H.J. Herman *et al.*, (eds.) *Supercomputing in Brain Research: From Tomography to Neural Networks*, World Scientific Pub. Corp. pp. 137–148, 1995.
21. T.W. Lee: *Independent Component Analysis: Theory and Applications* Kluwer Academic Publishers, ISBN: 0792382617, 1998.

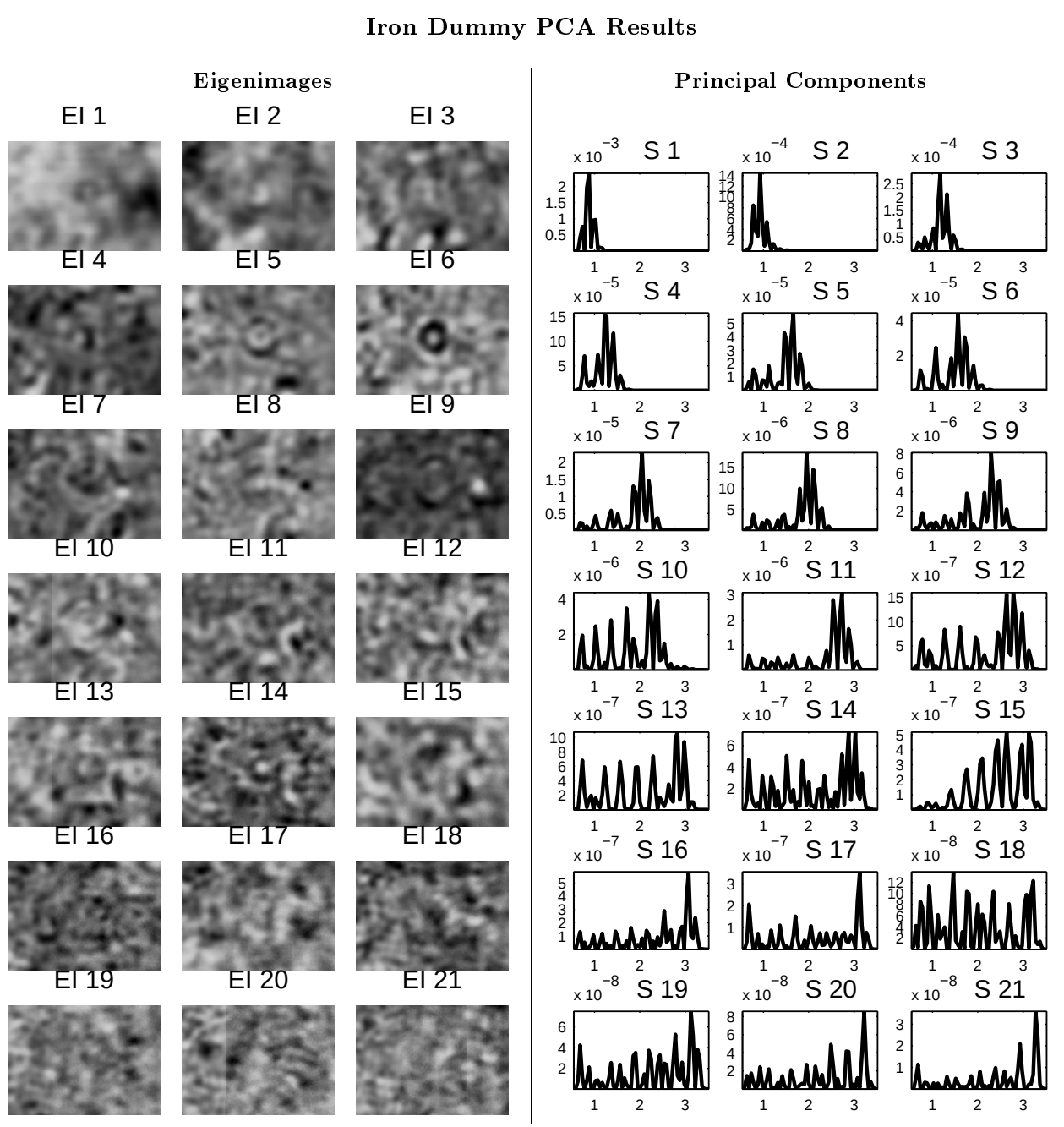


**Figure 1.** Eigenimages ($xy$-plane), $\boldsymbol{u}_i$, and associated PC's, $\boldsymbol{y}_i$, for the M56 iron dummy. Only the first $M = 21$ eigenimages and associated PC's are shown. It should be noticed that it is the power of the PC's that are shown. The power is calculated using a non-causal Kaiser window of size 3 with the characteristic parameter set to $2\pi$. The eigenimages shows very strong landmine signatures in a few eigenimages, e.g., eigenimage 5 and 6, and the associated PC's also peaks in a depth corresponding to the buried depth (1.8 nanosec.). Eigenimage 1, 2, and 3 and associated PC's shows strong ground surface signature. The eigenimages shows the variations in the ground surface and the associated PC's peaks at the ground surface (1.0 nansec.). The remaining eigenimages and PC's shows more mixed clutter-landmine signals. However, they have much less power. It is clear that the separation in time is poor. The eigenimages and PC's are used as inputs to the s-ICA and t-ICA.

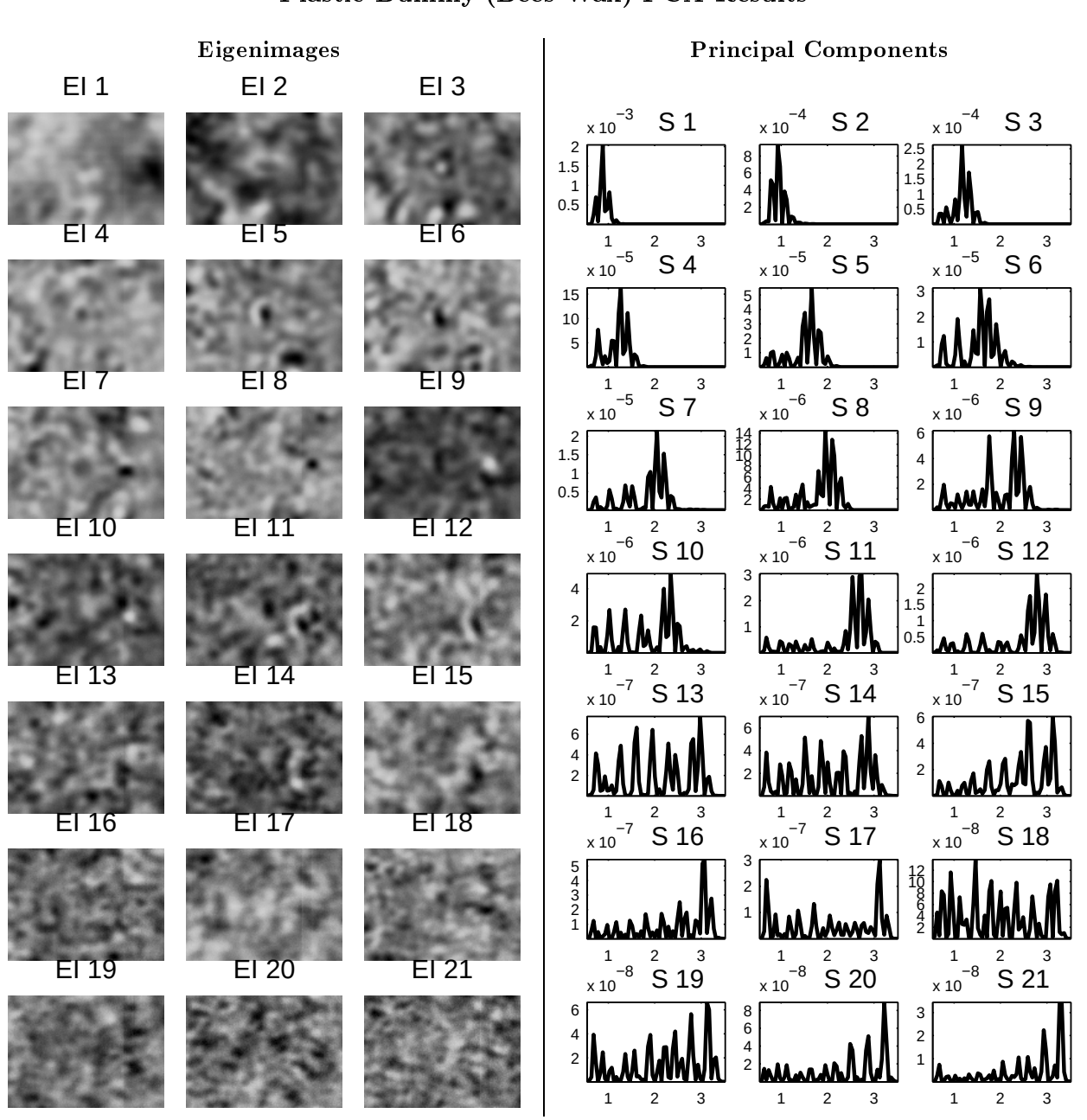


**Figure 2.** Eigenimages ($xy$-plane), $\boldsymbol{u}_i$, and associated PC's, $\boldsymbol{y}_i$, for the M56 plastic dummy (filled with bees wax). As for the M56 iron dummy, it is only the first $M = 21$ eigenimages and associated PC's that are shown. Again it should be noticed that it is the power of the PC's that are shown. The power is calculated using a non-causal Kaiser window of size 3 with the characteristic parameter set to $2\pi$. Due to the weak scattering from the plastic dummy the eigenimages shows very weak landmine signatures. However, eigenimage 5 and 6 shows landmine signatures, and the associated PC's also peaks in a depth corresponding to the buried depth (1.8 nanosec.). Eigenimage 1, 2, and 3 and associated PC's shows strong ground surface signature. The eigenimages shows the variations in the ground surface and the associated PC's peaks at the ground surface (1.0 nansec.). The remaining eigenimages and PC's shows more mixed clutter-landmine signals. However, they have much less power. It is clear that the separation in time is poor. The eigenimages and PC's are used as inputs to the s-ICA and t-ICA.

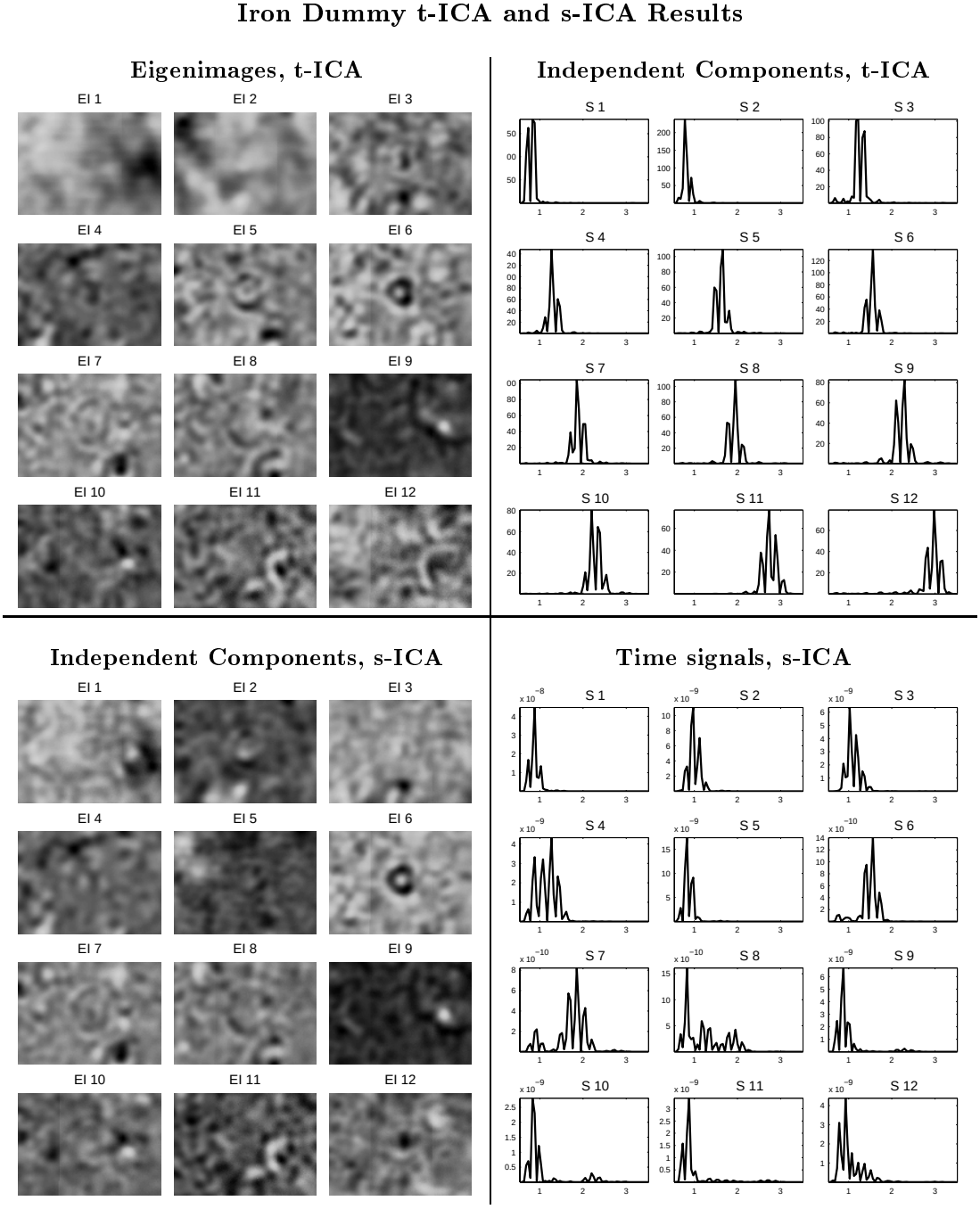


**Figure 3.** Eigenimages ($xy$-plane) and associated time signals for the t-ICA and the s-ICA having the first $M = 15$ PC's, $\boldsymbol{y}_i$, and eigenimages, $\boldsymbol{u}_i$, as input, respectively. Only the first eigenimages and time signals are shown. From the eigenimages and time signals it is clear that the t-ICA provides a good time separation, and the s-ICA provides a good spatial separation.

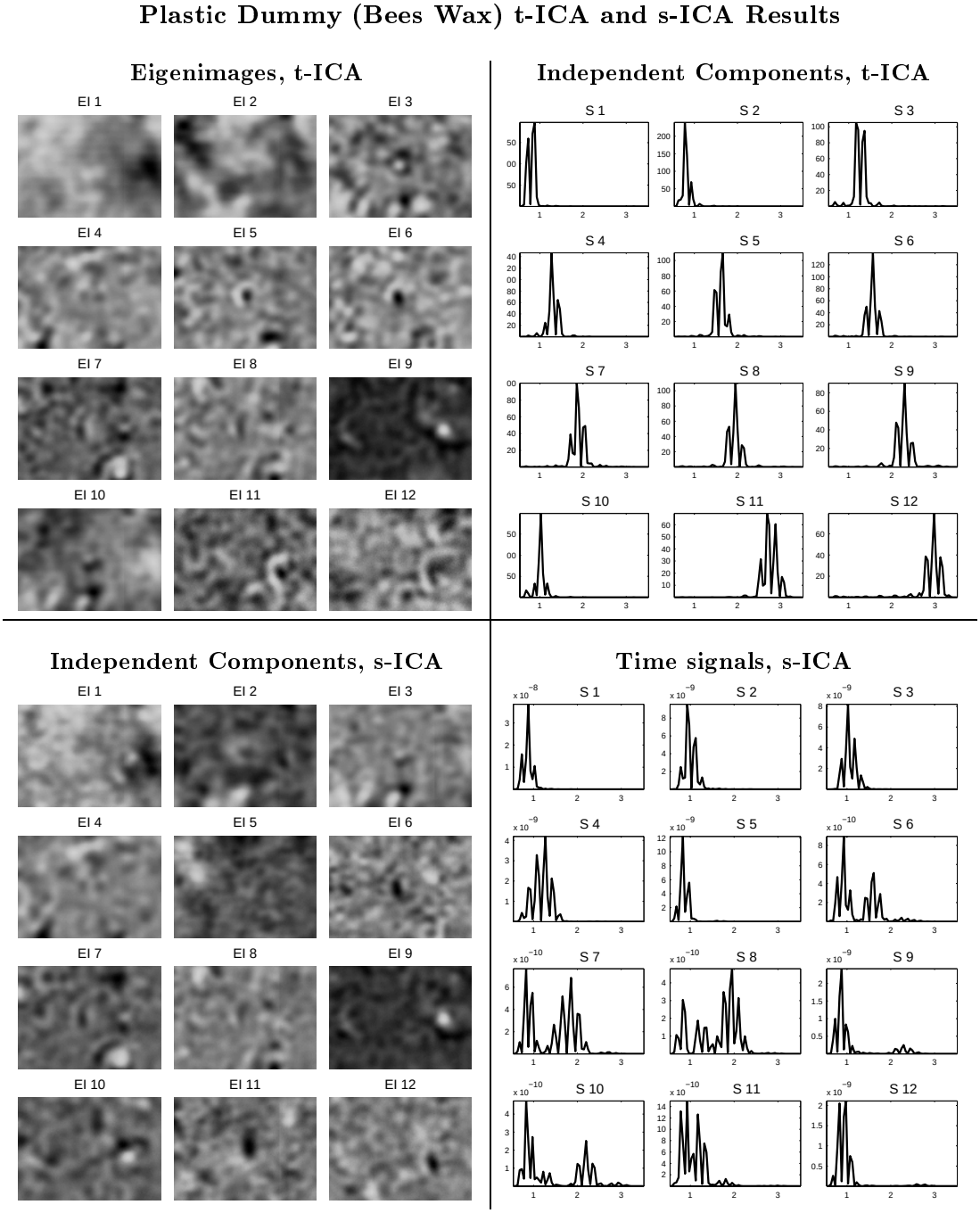


**Figure 4.** Eigenimages ($xy$-plane) and associated time signals for the t-ICA and the s-ICA having the first $M = 15$ PC's, $\boldsymbol{y}_i$, and eigenimages, $\boldsymbol{u}_i$, as input, respectively. Only the first eigenimages and time signals are shown. From the eigenimages and time signals it is clear that the t-ICA provides a good time separation, and the s-ICA provides a good spatial separation.


**Figure 5.** Reconstructed power images. In general, it is clear that the component selection method based on combined spatial and temporal features shows the best performance. The t-ICA and s-ICA are compared with the PCA method[11,12]. The t-ICA and in particular the s-ICA show both better performance than the PCA and the mean subtraction method. It should be noticed when using the component selection method based on temporal features the t-ICA shows best performance, and for the component selection method based on spatial features the s-ICA shows best performance. In overall, the s-ICA combined with the component selection method based on combined spatial and temporal features show the best performance. The landmine dummy is located in the center of each image.

## Iron Dummy Clutter Reduction Results

**a) Mean** **b) t-ICA, 15 PC's, Temp.**

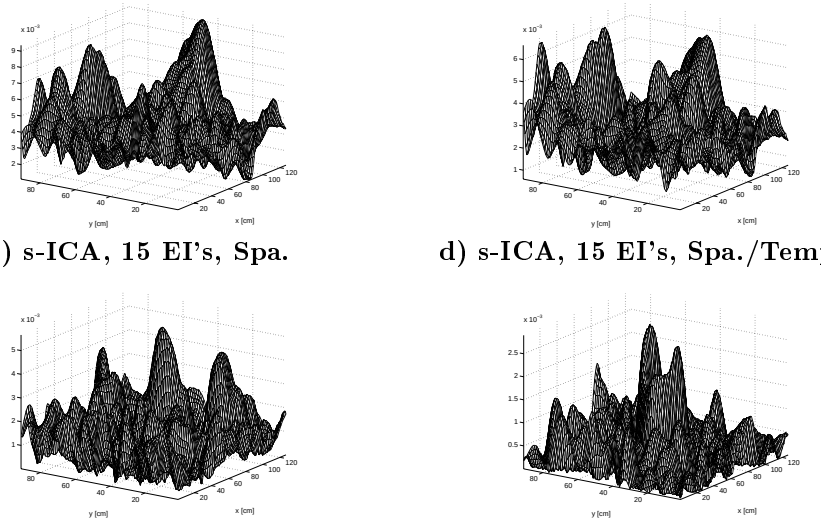

**c) s-ICA, 15 EI's, Spa.** **d) s-ICA, 15 EI's, Spa./Temp.**

**Figure 6.** **a**): mesh plot of mean-image. **b**): mesh plot of the t-ICA using 15 PC's as input and temporal feature component selection. **c**): mesh plot of the s-ICA using 15 EI's as input and spatial feature component selection. **d**): mesh plot of the s-ICA using 15 EI's as input and spatial/temporal feature component selection.

## Plastic Dummy (Bees Wax) Clutter Reduction Results

**a) Mean** **b) t-ICA, 15 PC's, Temp**

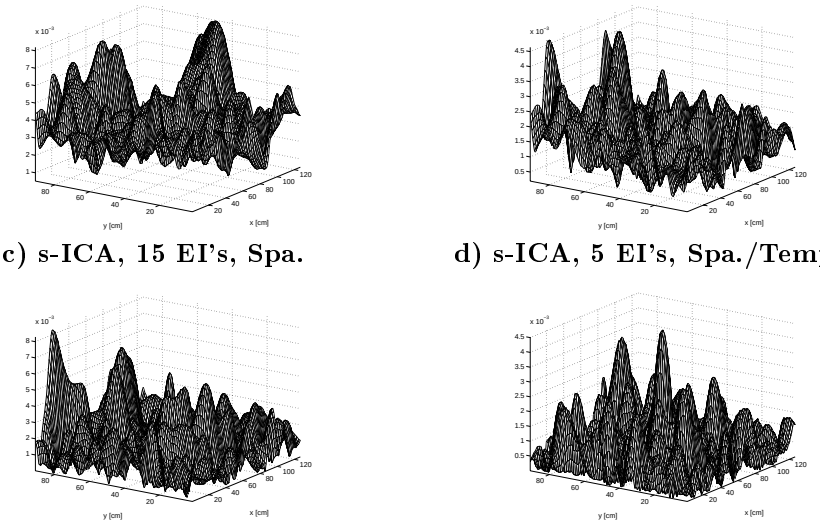

**c) s-ICA, 15 EI's, Spa.** **d) s-ICA, 5 EI's, Spa./Temp.**

**Figure 7.** **a**): mesh plot of mean-image. **b**): mesh plot of the t-ICA using 15 PC's as input and temporal feature component selection. **c**): mesh plot of the s-ICA using 15 EI's as input and spatial feature component selection. **d**): mesh plot of the s-ICA using 5 EI's as input and spatial/temporal feature component selection.